

# 1 Integrated transcriptomic, proteomic and epigenomic 2 analysis of *Plasmodium vivax* salivary-gland sporozoites.

3  
4 Vivax Sporozoite Consortium\* (Ivo Muller<sup>1,2,3</sup>, Aaron R. Jex<sup>1,3,4</sup>, Stefan H. I. Kappe<sup>5</sup>,  
5 Sebastian A. Mikolajczak<sup>5</sup>, Jetsumon Sattabongkot<sup>7</sup>, Rapatbhorn Patrapuvich<sup>6</sup>, Scott  
6 Lindner<sup>8</sup>, Erika L. Flannery<sup>5</sup>, Cristian Koepfli<sup>1</sup>, Brendan Ansell<sup>4</sup>, Anita Lerch<sup>1</sup>, Kristian  
7 Swearingen<sup>5</sup>, Robert Moritz<sup>9</sup>, Michaela Petter<sup>10</sup>, Michael Duffy<sup>10</sup>, Vorada Chuenchob<sup>5</sup>).

8 \*Group authorship – all others are equal contributors (order per author contributions section below).  
9

- 10 1. Population Health and Immunity Division, The Walter and Eliza Hall Institute for Medical Research, 1G Royal Parade,  
11 Parkville, Victoria, 3052, Australia.
- 12 2. Malaria: Parasites & Hosts Unit, Institut Pasteur, 28 Rue de Dr. Roux, 75015, Paris, France.
- 13 3. Department of Medical Biology, The University of Melbourne, Victoria, 3010, Australia.
- 14 4. Faculty of Veterinary and Agricultural Sciences, The University of Melbourne, Corner of Park and Flemington Road,  
15 Parkville, Victoria, 3010, Australia.
- 16 5. Center for Infectious Disease Research, 307 Westlake Avenue North, Suite 500, Seattle, WA 98109, USA;
- 17 6. Department of Global Health, University of Washington, Seattle, WA 98195, USA.
- 18 7. Mahidol Vivax Research Center, Faculty of Tropical Medicine, Mahidol University, Bangkok 10400, Thailand.
- 19 8. Department of Biochemistry and Molecular Biology, Center for Malaria Research, Pennsylvania State University, University  
20 Park, PA 16802, USA.
- 21 9. Institute for Systems Biology, Seattle, WA, 98109, USA.
- 22 10. Department of Medicine Royal Melbourne Hospital, The Peter Doherty Institute, The University of Melbourne, 792  
23 Elizabeth Street, Melbourne, Victoria 3000, Australia.

## 24 25 Abstract

26 **Background:** *Plasmodium vivax* is the key obstacle to malaria elimination in Asia and Latin  
27 America, largely attributed to its ability to form resilient ‘hypnozoites’ (sleeper-cells) in the  
28 host liver that escape treatment and cause relapsing infections. The decision to form  
29 hypnozoite is made early in the liver infection and may already be set in sporozoites prior to  
30 invasion. To better understand these early stages of infection, and the potential mechanisms  
31 through which the development may be pre-programmed, we undertook a comprehensive  
32 transcriptomic, proteomic and histone epigenetic characterization of *P. vivax* sporozoites.  
33

34 **Results:** Our study highlights the loading of the salivary-gland sporozoite with proteins  
35 required for cell traversal and invasion and transcripts for infection of and development  
36 within hepatocytes. We characterise histone epigenetic modifications in the *P. vivax*  
37 sporozoite and explore their role in regulating transcription. This work shows a close  
38 correlation between H3K9ac marks and transcriptional activity, with H3K4me3 and  
39 H3K9me3 appearing to act as general markers of euchromatin and heterochromatin  
40 respectively. We also identify the remarkable transcriptional silence in the (sub)telomeres and  
41 discuss potential roles of AP2 transcription factors, specifically ApiAP2-SP and L in  
42 regulating this stage.  
43

44 **Conclusions:** Collectively, these data indicate the sporozoite as a tightly programmed stage  
45 primed to infect the human host and identifies key targets to be further explored in liver stage  
46 models.  
47

## 48 Background

49 Malaria is among the most significant infectious diseases impacting humans globally, with  
50 3.3 billion people at risk of infection, 381 million suspected clinical cases and up to ~660,000  
51 deaths attributed to malaria globally in 2014 [1]. Two major parasite species contribute to the  
52 vast majority of human malaria, *Plasmodium falciparum* and *P. vivax*. Historically, *P.*  
53 *falciparum* has attracted the majority of global attention, due to its higher contribution to  
54 morbidity and mortality. However, *P. vivax* is broadly distributed, more pathogenic than  
55 previously thought, and is recognised as the key obstacle to malaria elimination in the Asia-  
56 Pacific and Americas [2]. Unlike *P. falciparum*, *P. vivax* can establish long-lasting ‘sleeper-  
57 cells’ (= hypnozoites) in the host liver that emerge weeks, months or years after the primary  
58 infection (= relapsing malaria) [3]. Primaquine is the only approved drug that prevents

59 relapse. However, the short half-life, long dosage regimens and incompatibility of primaquine  
60 with glucose-6-phosphate-dehydrogenase deficiency (which requires pre-screening of  
61 recipients [4]) makes it unsuitable for widespread use. As a consequence, *P. vivax* is  
62 overtaking *P. falciparum* as the primary cause of malaria in a number of co-endemic regions  
63 [5]. Developing new tools to diagnose, treat and/or prevent hypnozoite infections is  
64 considered one of the highest priorities in the malaria elimination research agenda [6].

65 When *Plasmodium* sporozoites are deposited by an infected mosquito, they likely  
66 traverse the skin cells, enter the blood-stream and are trafficked to the host liver, as has been  
67 shown in rodent malaria parasites [7]. Upon reaching the liver, sporozoites traverse Kupffer  
68 and endothelial cells to reach the parenchyma, moving through several hepatocytes before  
69 invading a final hepatocyte suitable for liver stage development [7, 8]. Within hepatocytes,  
70 these parasites replicate, and undergo further development and differentiation to produce tens  
71 of thousands of merozoites that emerge from the liver and infect red blood cells. However, *P.*  
72 *vivax* sporozoites are able to commit to two distinct developmental fates within the  
73 hepatocyte: they either immediately continue development as replicating schizonts and  
74 establish a blood infection, or delay replication and persist as hypnozoites. Regulation of this  
75 major development fate decision is not understood and this represents a key gap in current  
76 knowledge of *P. vivax* biology and control.

77 The sporozoites' journey from skin deposition to hepatocytes takes less than a few  
78 minutes [9]. It has been hypothesized that *P. vivax* sporozoites exist within an inoculum as  
79 replicating 'tachysporozoites' and relapsing 'bradysporozoites' [10] and that these  
80 subpopulations may have distinct developmental fates as schizont or hypnozoites, thus  
81 contributing to their relapse phenotype [10-12]. This observation is supported by the stability  
82 of different hypnozoite phenotypes in *P. vivax* infections of liver-chimeric mouse models  
83 [13]. Sporozoites prepare for mammalian host infection while still residing in the mosquito  
84 salivary glands. Studies using rodent malaria parasites have identified genes [14], that are  
85 transcribed in sporozoites but translationally repressed (i.e., present as transcript but un- or  
86 under-represented as protein), via RNA-binding proteins [15], and ready for just-in-time  
87 translation after the parasites infection of the mammalian host [13, 16]. Translational  
88 repression (i.e., the blocking of translation of present and retained transcripts) and other  
89 mechanisms of epigenetic control may contribute to the *P. vivax* sporozoite fate decision and  
90 hypnozoite formation, persistence and activation. Supporting this hypothesis, histone  
91 methyltransferase inhibitors stimulate increased activation of *Plasmodium cynomolgi*  
92 hypnozoites in macaque hepatocytes [17, 18]. Epigenetic control of stage development is  
93 further evidenced in *Plasmodium* through chromatin structure controlling expression of  
94 PfAP2-G, a specific transcription factor that, in turn, regulates gametocyte (dimorphic sexual  
95 stages) development in blood-stages [19]. It is well documented that *P. vivax* hypnozoite  
96 activation patterns stratify with climate and geography [11] and recent modelling suggests  
97 transmission potential selects for hypnozoite phenotype [20]. Clearly the ability for *P. vivax*  
98 to dynamically regulate hypnozoite formation and relapse phenotypes in response to high or  
99 low transmission periods in different climate conditions would confer a significant  
100 evolutionary advantage.

101 Unfortunately, despite recent advances [21] current approaches for *in vitro P. vivax*  
102 culture do not support routine maintenance in the laboratory and tools to directly perturb gene  
103 function are not established. This renders studies on *P. vivax*, particularly its sporozoites and  
104 liver stages, exceedingly difficult. Although *in-vitro* liver stage assays and humanised mouse  
105 models are being developed [13], they cannot yet support 'omics analysis of *P. vivax* liver  
106 stage dormancy. Recent characterization [22] of liver-stage (hypnozoites and schizonts) of *P.*  
107 *cynomolgi* (a related and relapsing parasite in macaques) provides valuable insight, but  
108 investigations in *P. vivax* directly are clearly needed. The systems analysis of *P. vivax*  
109 sporozoites that reside in the mosquito salivary glands and are poised for transmission and  
110 liver infection offer a key opportunity to gain insight into *P. vivax* infection. To date, such  
111 characterization of *Plasmodium vivax* sporozoites is limited [23], and only one recent study,  
112 of *P. falciparum* [24], has undertaken exploration of epigenetic regulation in sporozoites of  
113 any *Plasmodium* species. Here, we present a detailed characterization of the *P. vivax*

114 sporozoite transcriptome, proteome and epigenome and use these data to better understand  
115 this key infective stage and the role of sporozoite programming in invasion and infection of  
116 the human host, and development within the host liver.

117

## 118 **Results and Discussion**

119 We quantified transcript abundance for 5,714 *P. vivax* genes (4,991 with a mean transcript per  
120 million (TPM) count  $\geq 1.0$ ) at a mean estimated abundance of 175.1 TPM (Additional File 1:  
121 Figure S1 and Additional File 2: Table S1) for *P. vivax* sporozoites isolated from *Anopheles*  
122 *dirus* salivary glands using the recently completed *P. vivax* P01 assembly and gene models  
123 (see methods). For ease of reference, where one-to-one orthologs are established between the  
124 P01 and previous *P. vivax* (Sal1) reference, we use the Sal1 gene names in text (both the P01  
125 and Sal1 gene names are provided for all genes in the supplementary information). Mosquito  
126 infections were generated by membrane feeding of blood samples taken from *P. vivax*  
127 infected patients in western Thailand (n = 9). Among the most highly transcribed genes in the  
128 infectious sporozoite stage are *csp* (circumsporozoite protein), five *etramps* (early transcribed  
129 membrane proteins), including *uis3* (up-regulated in infective sporozoites), *uis4* and *lsap-1*  
130 (liver stage associated protein 1), a variety of genes involved in cell transversal and initiation  
131 of invasion, including *celtos* (cell traversal protein for ookinetes and sporozoites), *gest*  
132 (gamete egress and sporozoite traversal protein), *spect1* (sporozoite protein essential for cell  
133 traversal) and *siap-1* (sporozoite invasion associated protein), and genes associated with  
134 translational repression (*alba1*, *alba4* and *Puf2*). Collectively, these genes account for  $>1/3^{\text{rd}}$   
135 of all transcription in the sporozoite. We found moderate agreement ( $R^2 = 0.35$ ; Additional  
136 File 1: Figure S2) between our RNA-seq data and previous microarray data for *P. vivax*  
137 sporozoites [23]. Improved transcript detection and quantitation is expected with the  
138 improved technical resolution of RNA-seq over microarray. Supporting this, we find higher  
139 correlation between RNA-seq data from *P. vivax* and *P. falciparum* (single replicate  
140 sequenced herein for comparative purposes) sporozoite datasets ( $R^2 = 0.42$ ), compared to  
141 either species relative to published microarray data (Additional File 1: Figure S2). Although  
142 microarray supports the high transcription in sporozoites of genes such as *uis4*, *csp*, *celtos* and  
143 several other *etramps*, 27% and 16% of the most abundant 1% of transcribed genes in our  
144 sporozoite RNA-seq data are absent from the top decile or quartile respectively in the existing  
145 *P. vivax* sporozoite microarray data [23]. Among these are genes involved in early  
146 invasion/hepatocyte development, such as *lsap-1*, *celtos*, *gest* and *siap-1*, or translational  
147 repression (e.g., *alba-1* and *alba-4*); orthologs of these genes are also in the top percentile of  
148 transcripts in RNA-seq (see [24] and Additional File 2: Table S2) and (see [25] and  
149 Additional File 2: Table S3) and previous microarray data [26, 27] for *P. falciparum* and *P.*  
150 *yoelii* sporozoites respectively, suggesting many are indeed more abundant than previously  
151 characterized.

152

### 153 **Transcription in *P. vivax* relative to other plasmodia**

154 To gain insight into species-specific aspects of the *P. vivax* transcriptome, we qualitatively  
155 compared these data with available data from *P. falciparum* and *P. yoelii* sporozoites (single  
156 replicate only) for 4,220 and 4,067 single-copy orthologs (SCO) (transcribed at  $\geq 1$  TPM in *P.*  
157 *vivax* infectious sporozoites) shared with *P. falciparum* (Additional File 2: Table S3) and with  
158 both *P. falciparum* and *P. yoelii* (Additional File 2: Table S4) respectively. Genes highly  
159 transcribed in salivary-gland sporozoites of all three species include *celtos*, *gest*, *trap*, *siap1*,  
160 *spect1* and *puf2*. There are 696 *P. vivax* genes shared as orthologs between *P. vivax* P01 and  
161 *P. vivax* Sal1 lacking a defined SCO in *P. falciparum* or *P. yoelii* transcribed at a mean of  $\geq 1$   
162 TPM in *P. vivax* salivary-gland sporozoites (Additional File 2: Table S5). Prominent among  
163 these are *vir* (n=25) and *Pv-fam* (41 fam-e, 16 fam-b, 14 fam-a, 8 fam-d and 3 fam-h) genes,  
164 as well as, hypothetical proteins or proteins of unknown function (n=212) and, interestingly, a  
165 number of ‘merozoite surface protein’ 3 and 7 homologs (n=5 of each). Both *msp3* and *msp7*  
166 have undergone significant expansion in *P. vivax* relative to *P. falciparum* and *P. yoelii* [28]  
167 and may have repurposed functions in sporozoites. In addition, there are 69 *P. vivax* P01

168 genes lacking a defined ortholog in *P. vivax* Sal1, *P. falciparum* or *P. yoelli* transcribed at  $\geq 1$   
169 TPM in infectious *P. vivax* sporozoites; most of which are *Plasmodium* interspersed repeat  
170 (PIR) genes [28] found in telomeric regions of the P01 assembly and likely absent from the  
171 Sal1 assembly but present in the Sal1 genome.

172

### 173 ***P. vivax* sporozoite transcriptional enrichment**

174 To comprehensively identify sporozoite enriched transcripts, we compared the *P. vivax*  
175 sporozoite transcriptome (Additional File 2: Table S6) to RNA-seq data for *P. vivax* blood-  
176 stages [29] (the only other RNA-seq data presently available for *P. vivax*; Fig. 1 and  
177 Additional File 1: Figures S3-5). We identified 1,672 up (Additional File 2: Table S7) and  
178 1,958 down-regulated (Additional File 2: Table S8) transcripts ( $FDR \leq 0.05$ ; minimum 2-fold  
179 change in Counts per Million (CPM)) and next explored patterns among these differentially  
180 transcribed genes (DTGs) by protein family (Fig. 1C and Additional File 2: Table S9) and  
181 Gene Ontology (GO) classifications (Additional File 2: Table S10). RNA recognition motifs  
182 (RRM-1 and RRM-6) and helicase domains (Helicase-C and DEAD box helicases) are over-  
183 represented ( $p$ -value  $< 0.05$ ) among sporozoite-enriched transcripts, consistent with  
184 translational repression through ribonucleoprotein (RNP) granules [30]. Transcripts encoding  
185 nucleic acid binding domains, such as bromodomains (PF00439; which can also bind lysine-  
186 acetylated proteins), zinc fingers (PF13923) and EF hand domains (PF13499) are also  
187 enriched in sporozoites. Included among these proteins are a putative ApiAP2 transcription  
188 factor (PVX\_083040) and a homologue of the *Drosophila* zinc-binding protein ‘Yippee’  
189 (PVX\_099695). Thrombospondin-1 like repeats (TSR: PF00090) and von Willebrand factor  
190 type A domains (PF00092) are enriched in sporozoites as well. In sporozoites, *P. falciparum*  
191 genes enriched in TSR domains are important in invasion of the mosquito salivary gland (e.g.,  
192 *trap*) and secretory vesicles released by sporozoites upon entering the vertebrate host (e.g.,  
193 *msp*) [31]. By comparison, genes up-regulated in blood-stages are enriched for *vir* gene  
194 domains (PF09687 and PF05796), Tryptophan-Threonine-rich *Plasmodium* antigens  
195 (PF12319; which are associated with merozoites [32]), markers of cell-division  
196 (PF02493), [33] protein production/degradation (PF00112, PF10584, PF00152, PF09688 and  
197 PF00227) and ATP metabolism (PF08238 and PF12774). 47 of the 343 transcripts unique to  
198 *P. vivax* sporozoites relative to *P. falciparum* or *P. yoelli* are enriched in sporozoites  
199 compared to *P. vivax* blood stages. Nine of these are in the top decile of transcription, and  
200 include a Pv-fam-e (PVX\_089880), a Pf-fam-b homolog (PVX\_001710) and 7 proteins of  
201 unknown function. A further nine have an ortholog in *P. cynomolgi* (which also forms  
202 hypnozoites) but not the closely related *P. knowlesi* (which does not form hypnozoites) and  
203 include ‘*msp7*’-like (PVX\_082685, PVX\_082650 and PVX\_082670) and ‘*msp3*’-like  
204 (PVX\_097705) and Pv-fam-e genes (PVX\_001100, PVX\_089860 and PVX\_089810), a  
205 serine-threonine protein kinase (PVX\_081395) and a RecQ1 helicase homolog  
206 (PVX\_099345). Notably, the *P. cynomolgi* ortholog of PVX\_081395, PCYB\_021650, is  
207 transcriptionally enriched in hypnozoites relative to replicating schizonts [22], indicating a  
208 target of significant interest when considering hypnozoite formation and/or biology.

209

### 210 **Translational repression machinery**

211 In *Plasmodium*, translational repression regulates key life-cycle transitions coinciding with  
212 switching between the mosquito and the mammalian host (either as sporozoites or  
213 gametocytes) [30]. For example, although *uis4* is the most abundant transcript in the  
214 infectious sporozoite ([23, 27]; Additional File 2: Table S1), UIS4 is translationally repressed  
215 in this stage [15] and only expressed after hepatocyte invasion [34]. In sporozoites, it is  
216 thought that PUF2 binds to mRNA transcripts and prevents their translation [25], and SAPI  
217 stabilises the repressed transcripts and prevents their degradation [34]. Consistent with this,  
218 *Puf2* and *SAPI1* are among the more abundant *P. vivax* transcripts enriched in the sporozoite  
219 relative to blood-stages. Indeed, *Puf2* is among the top percentile of transcripts in infectious  
220 sporozoites. However, our data implicate other genes, many already known to be involved in  
221 translational repression in other *Plasmodium* stages and other protists [30], that may act in *P.*  
222 *vivax* sporozoites. Notable among these are *alba-2* and *alba-4*, both of which are among the

223 top 2% of genes transcribed in sporozoites and ~14 to 20-fold more highly transcribed in  
224 sporozoites relative to blood-stages. In addition, *P. vivax* sporozoites are enriched for genes  
225 encoding RRM-6 RNA helicase domains. Intriguing among these genes are HoMu (homolog  
226 of Musashi) and ptbp (polypyrimidine tract binding protein). Musashi is a master regulator of  
227 eukaryotic stem cell differentiation through translational repression [35] and HoMu localizes  
228 with DOZI and CITH in *Plasmodium* gametocytes [36]. PTBP is linked to mRNA stability,  
229 splice regulation and translational initiation [37] and may perform a complementary role to  
230 SAP1.

231

### 232 **Translational repression in *P. vivax* sporozoites**

233 More than 700 genes have been identified as being translationally repressed in *Plasmodium*  
234 *berghei* ('rodent malaria') gametocytes based on DOZI pulldowns [38]. In contrast,  
235 translationally repressed genes have not been characterized in sporozoites in a comprehensive  
236 way. As a step in addressing this, we analysed the *P. vivax* sporozoite proteome (Additional  
237 File 1: Figure S6 and Additional File 2: Table S11) by mass spectrometry and identified  
238 peptide signals for 2,640 proteins. Among the most highly expressed proteins in sporozoites  
239 were those associated with the apical complex (AMA1, GAMA, RON12, RON3, RON5),  
240 motility / cell traversal (MYOSIN A, PLP1, TRAP, SIAP1, GEST, SPECT1, CELTOS) and  
241 the inner membrane complex (ISP1/3, IMC1a, e, g, h, m and k), which has a key role in  
242 motility and invasion [39]. We identified 2,402 *P. vivax* genes transcribed in the sporozoite  
243 (TPKM > 1) for which no protein expression was detected. In considering genes that may be  
244 translational repressed (i.e., transcribed but not translated) in the *P. vivax* sporozoite, we  
245 confine our observations to those transcripts representing the top decile of transcript  
246 abundance to ensure their lack of detection as proteins was not due to limitations in the  
247 detection sensitivity of the proteomic dataset. Notably, ~1/3<sup>rd</sup> of transcripts in the top decile  
248 of transcriptional abundance (n = 173 of 558) in *P. vivax* sporozoites were not detectable as  
249 peptides in multiple replicates (Additional File 2: Table S12). Of these 173 putatively  
250 repressed transcripts, 156 and 154 have orthologs in *P. falciparum* and *P. yoelii* respectively,  
251 with 89 and 118 of these also not detected as proteins in *P. falciparum* and *P. yoelii* salivary-  
252 gland sporozoites [40] despite being identified as transcribed in these stages (see [24, 25];  
253 Additional File 2: Tables S2-4). In addition, a number of genes (e.g., *uis4*) are expressed in  
254 infectious *P. vivax* sporozoites at levels many fold lower than their transcription might  
255 indicate (bottom quartile of protein expression, compared with top decile of transcript  
256 abundance). While each putatively repressed transcript will require validation, this system  
257 level approach is supported by immunofluorescent imaging (Additional File 1: Figure S7) of  
258 UIS4 and LISP1 (one known and one proposed here as translationally repressed in *P. vivax*  
259 sporozoites) relative to TRAP and BiP (which are both transcribed and expressed as protein in  
260 the *P. vivax* sporozoite; Additional File 2: Table S12).

261

### 262 *Development within the host hepatocyte*

263 Following cell traversal and hepatocyte invasion, *P. vivax* sporozoites establish their  
264 intracellular niche, which includes modification of the parasitophorous vacuole membrane  
265 (PVM) and the parasite then proceeds to replicate as a liver stage. UIS3 and UIS4 are resident  
266 PVM-proteins and are the best characterized proteins under translational repression by  
267 Puf2/SAP1 in infectious sporozoites [41], both of which are essential for liver stage  
268 development [14]. In the present study, *uis4* represents 18.8% of transcripts but just 0.06% of  
269 proteins in the sporozoites. Similarly, *uis3* is the 7<sup>th</sup> most abundant transcript in sporozoites,  
270 but represented only by a single peptide count in one proteomic replicate. In addition to *uis3*  
271 and *uis4*, genes involved in liver stage development and under apparent translational  
272 repression in the *P. vivax* sporozoites include *lsapl* (liver stage associated protein 1), *zipco*  
273 (ZIP domain-containing protein), several other *etramps* (PVX\_118680, PVX\_003565,  
274 PVX\_088870 and PVX\_086915), *pv1* (parasitophorous vacuole protein 1) and *lisp1* and *lisp2*  
275 (PVX\_085550 and PVX\_000975). The *lisp1* gene is an intriguing find, and may have an  
276 altered role in *P. vivax* liver stages (Additional File 1: Figure S7). In *P. berghei*, *lisp1* is  
277 essential for rupture of the PVM during liver stage development allowing release of the

278 merozoite into the host blood stream. *Pv-lispl* is ~350-fold and ~1,350-fold more highly  
279 transcribed in *P. vivax* sporozoites compared to sporozoites of either *P. falciparum* or *P.*  
280 *yoelli* (see Additional File 2: Table S4). Also notable among translationally repressed genes in  
281 sporozoites is a putative ‘Yippee’ homolog (PVX\_099695). Yippee is a DNA-binding protein  
282 that, in humans (YPEL3), suppresses cell growth [42]. Its specific function in *Plasmodium*,  
283 either in parasite development or on the host interactions, is not yet known. However, that  
284 Yippee-like proteins suppress cell growth/division and appear to be regulated through histone  
285 acetylation [43] is intriguing in the context of a potential role in *P. vivax* hypnozoite  
286 developmental arrest.

287 The *P. vivax* ortholog (PVP01\_1016100; no corresponding ortholog is identified in  
288 the *P. vivax* Sal1 assembly) of the *P. cynomolgi* AP2 transcription factor, PCYB\_102390,  
289 which was recently designated AP2-Q (i.e., ‘quiescent’) due to its enriched transcription in *P.*  
290 *cynomolgi* hypnozoites [22], is also detectable as transcripts but not proteins in *P. vivax*  
291 sporozoites. This may support a specific role for this transcription factor in hypnozoites.  
292 However, as Pv-AP2-Q is transcribed at an abundance (~50 TPM) at or below which ~≥50%  
293 of *P. vivax* genes are detectable as transcripts but not as proteins, the lack of detected AP2-Q  
294 protein could as likely result from the detection sensitivity of the proteomics data-set as from  
295 translation repression. Furthermore, while AP2-Q is proposed in *P. cynomolgi* as a possible  
296 hypnozoite marker in part due to its presence in *P. cynomolgi*, *P. vivax* and *P. ovale* (all of  
297 which generate hypnozoites) and reported absence from other *Plasmodium* species [22].  
298 However, orthologs of this gene are also identified in PlasmoDB for several non-hypnozoite  
299 producing *Plasmodium* species, such as *P. knowlesi*, *P. gallinaceum* and *P. inui*, raising  
300 questions in regard to its function in these parasite species.

301 Lastly, while *Plasmodium* species lack a classical Golgi body, some genes (e.g., *golgi*  
302 *reassembly stacking protein*) functioning in protein transport between the Golgi body and the  
303 endoplasmic reticulum have been repurposed for vesicular transport and protein secretion  
304 during invasion [44]. Noting this, several homologs of genes associated with cycling of  
305 proteins between the Golgi body and the ER in other eukaryotes, including COPI-associated  
306 protein (PVX\_100850), a putative STF2 (PVX\_116780) and Got1 (PVX\_090050) appear  
307 under translational repression in *P. vivax* sporozoites. Interestingly, in liver cells, the  
308 membrane of the parasitophorous vacuole, in which *Plasmodium* resides, often associates  
309 with the host cell ER and Golgi apparatus and may exploit this association to hijack host  
310 secretory pathways [45]. This may represent a key mechanism underpinning development in  
311 hepatocytes meriting further study.

312

### 313 *Apoptosis-inhibition*

314 Also notable among genes apparently translationally repressed in sporozoites are two putative  
315 Bax1 (Bcl-2 associated X protein) inhibitors (PVX\_117470 and PVX\_101315). Bax1  
316 dimerizes with Bcl-2 to promote intrinsic apoptosis, leading to destruction of the  
317 mitochondrial membrane, caspase release and cell death. Bax1 inhibitor is a component of the  
318 cell stress response to prevent Bax1 from prematurely triggering cell death. When Bax1 is  
319 blocked, Bcl-2 switches from a cell-death to a pro-survival/anti-apoptotic role [46].  
320 Intriguingly, specific suppression of mitochondrial-induced apoptosis has been demonstrated  
321 in liver-cells infected with *P. yoelii* [47] and this anti-apoptotic signal is blocked by Bcl-2  
322 family inhibitors [48]. Orthologs of both *P. vivax* encoded Bax1 inhibitors are found in all  
323 *Plasmodium* species, suggesting a conserved function across the genus. Nonetheless, it is  
324 attractive to contemplate a potential role for these genes in promoting survival of host  
325 hepatocytes following the initial parasite invasion. Notably, the *P. cynomolgi* orthology of  
326 PVX\_101315, PCYB\_147290, is ~2-fold enriched in transcript abundance in schizonts  
327 compared to hypnozoites, which may indicate a role in repressing hepatocyte cell death  
328 during parasite replication rather than extending its life-span during parasite dormancy. This  
329 is to be explored.

330

### 331 **Potential binding motif for Pv-Puf2**

332 Research in *Toxoplasma gondii*, has identified a repetitive UGU motif in coding regions of  
333 translationally repressed genes bound by *Tg*-Puf2 [49] and, presumably, mediating repression.  
334 A similar UGU motif has been identified in the 3'UTR of *P. falciparum* transcripts (e.g.,  
335 pfs25 and pfs28) and shown to bind PfPUF2 leading to their translational repression [50]. The  
336 binding motif for *Pv*-PUF2 has not been described. We found one motif (AGAT[TAC]G;  
337 Additional File 1: Figure S8) over-represented in coding regions of putatively repressed  
338 sporozoite transcripts relative to similarly highly transcribed but also translated genes e-value:  
339  $1.9e^{-9}$ ). We note the complementarity between AGAT and UGUA, however no over-  
340 represented motifs were detected in the 3'UTRs of these genes. Intriguingly, translational  
341 repression of *uis4* in *P. berghei* does not require the UTR [15]. It may be that the location of  
342 the *Puf2*-binding motif is somewhat flexible in *Plasmodium* and other apicomplexan  
343 species. We also identified a similarly over-represented motif ([GT]CGTC[CT]) within  
344 500bp upstream of putatively repressed genes (p-value:  $2.2e^{-9}$ ). It is possible this motif is a  
345 binding site for an as yet unattributed transcription factor co-ordinating genes destined for  
346 translational repression in the sporozoite. This motif is comparable to the [AG]C[AG]TGC  
347 motif identified for Pf-AP2-Sp [24], a transcription factor that is required for sporozoite  
348 development in *P. berghei* [51], and transcriptionally enriched in *P. falciparum* [24] and *P.*  
349 *vivax* (Additional File 2: Table S7) sporozoites relative to oocysts or blood stages  
350 respectively.

351

### 352 **Histone modifications in *P. vivax* sporozoites**

353 No epigenetic data are currently available for any *P. vivax* life-cycle stage. Studies of *P.*  
354 *falciparum* blood-stages have identified the importance of histone modifications as a primary  
355 epigenetic regulator [52, 53] and characterized key markers of heterochromatin (H3K9me<sup>3</sup>)  
356 and euchromatin/transcriptional activation (H3K4me<sup>3</sup> and H3K9ac). Recently, these marks  
357 have been explored with the maturation of *P. falciparum* sporozoites in the mosquito [24].  
358 Here, we characterize these marks in *P. vivax* sporozoites and assess their relationship to  
359 transcript abundance. Clearly this is of particular interest as a potential mechanism for  
360 dynamic regulation of sporozoite development in human hepatocytes. We identified 1,506,  
361 1,999 and 5,262 ChIP-seq peaks stably represented in multiple *P. vivax* sporozoite replicates  
362 and associated with H3K9me<sup>3</sup>, H3K9ac and H3K4me<sup>3</sup> histone marks respectively (Fig. 2).  
363 Peak width, spacing and stability differed with histone mark type (Additional File 1: Figures  
364 S9 and S10). H3K4me<sup>3</sup> peaks were significantly broader (mean width: 1,985 bp) than H3K9  
365 peaks, and covered the greatest breadth of the genome; 36.0% of all bases were stably  
366 associated with H3K4me<sup>3</sup> marks. This mark was also most stable among replicates, with just  
367 ~16% of bases associated with an H3K4me<sup>3</sup> not supported by more than one biological  
368 replicate. By comparison H3K9me<sup>3</sup> marks were narrowest (mean width: 796 bp) and least  
369 stable, with 46% of bases associated with this mark supported by just one replicate.  
370 Consistent with observations in *P. falciparum* H3K9me<sup>3</sup> 'heterochromatin' marks primarily  
371 clustered in telomeric and subtelomeric regions (Additional File 1: Figure S11). In contrast,  
372 the 'euchromatin' / transcriptionally open histone marks, H3K4me<sup>3</sup> and H3K9ac clustered  
373 around genic regions and did not overlap with regions under H3K9me<sup>3</sup> suppression. Both  
374 H3K9me<sup>3</sup> and H3K4me<sup>3</sup> marks were reasonably uniformly distributed (mean peak spacing  
375 ~500bp for each) within their respective regions of the genome. In contrast, H3K9ac peaks  
376 were spaced farther apart (mean: ~2kb), but also with a greater variability in spacing (likely  
377 reflecting their association with promoter regions [54]). The instability of H3K9me<sup>3</sup> may  
378 reflect its use in *Plasmodium* for regulating variegated expression of contingency genes from  
379 multigene families whose members have overlapping and redundant functions [55] and confer  
380 phenotypic plasticity [56].

381

### 382 *Genes under histone regulation*

383 We explored an association between these histone marks and the transcriptional behaviour of  
384 protein coding genes (Fig. 2 and Additional File 2: Tables S13-17). 485 coding genes stably  
385 intersected with an H3K9me<sup>3</sup> mark; all are located near the ends of the chromosomal  
386 scaffolds (i.e., are (sub)telomeric). On average, these genes are transcribed at ~30 fold lower

387 levels (mean <3 TPKMs) than genes not stably intersected by H3K9me<sup>3</sup> marks. These data  
388 clearly support the function of this mark in transcriptional silencing. This is largely consistent  
389 with observations in *P. falciparum* sporozoites [24], however, we observe no instances of  
390 genes that are stably marked by H3K9me<sup>3</sup> and moderately or highly transcribed regardless.  
391 Whether this relates to differences in epigenetic control between the species is not clear. We  
392 note that (sub)telomeric genes are overall transcriptionally silent in *P. vivax* sporozoites  
393 relative to blood-stages (Fig. 2a and 2b and Additional File 2: Tables S18-20). Consistent  
394 with observations in *P. falciparum* [52], the bulk of these genes include complex protein  
395 families, such as *vir* and *Pv-fam* genes, which function primarily in blood-stages. Also  
396 notable among the genes are several reticulocyte-binding proteins, including RBP2, 2a, 2b  
397 and 2c. Strikingly, we find no exceptions to this trend in our data, indicating the  
398 (sub)telomeres are remarkably transcriptionally silent in the sporozoite stage. By comparison,  
399 H3K4me<sup>3</sup> marks are stably associated with the Transcription Start Site (TSS) and/or 5' UTRs  
400 of 3,677 genes. We also identified 1,284 coding genes stably associated with an H3K9ac  
401 mark within 1kb of the TSS, with 179 of these genes stably marked also by H3K4me<sup>3</sup>. The  
402 average transcription of these genes is 116, 180 and 199 TPKMs respectively (39, 60 and 66-  
403 fold higher than H3K9me<sup>3</sup> marked genes). These data support the role of these marks in  
404 transcriptional activation, the lower abundance of H3K4me<sup>3</sup> marker, compared with H3K9ac  
405 or H3K9ac and H3K4me<sup>3</sup> marked genes suggest these marks work synergistically and that  
406 H3K9ac is possibly the better single mark indicator of transcriptional activity in *P. vivax*. This  
407 is consistent with recent observations in *P. falciparum* sporozoites [24].

408 Interestingly, H3K9ac-marked genes ranged in transcriptional activity from the most  
409 abundantly transcribed genes to many in the lower 50% and even lowest decile of  
410 transcription. This suggests more contributes to transcriptional activation in *P. vivax* than,  
411 simply, gene accessibility through chromatin regulation. Specific activation by a transcription  
412 factor (e.g., ApiAP2s [57]) is the most obvious candidate. To explore this, we compared  
413 upstream regions (within 1kb of the TSS or up to the 3' end of the next gene upstream,  
414 whichever was less) of highly (top 10%) and lowly (bottom 10%) transcribed H3K9ac  
415 marked genes for over-represented sequence motifs that might coincide with known ApiAP2  
416 transcription factor binding sites [58]. We identified these based on the location of the nearest  
417 stable H3K9ac peak relative to the transcription start site for each gene (Additional File 1:  
418 Figure S12). In most instances, these peaks were within 100bp of the TSS and, consistent  
419 with data from *P. falciparum* [54], *P. vivax* promoters appear to be no more than a few  
420 hundred to a maximum of 1000 bp upstream of the TSS. Exploring these regions, we  
421 identified two over-represented motifs: TGTACMA (e-value  $2.7e^{-2}$ ) and ATATTTH (e-value  
422  $3.3e^{-3}$ ) (Fig. 2D). TGTAC is consistent with the known binding site for *Pf*-AP2-G, which  
423 regulates sexual differentiation in gametocytes [59], but its *P. vivax* ortholog (PVX\_123760)  
424 is neither highly transcribed nor expressed in sporozoites. It may be that some genes encoding  
425 this domain are active in both sporozoites and gametocytes, but regulated by different  
426 mechanisms in each stage. Alternatively, this motif may represent a binding site for another,  
427 as yet uncharacterized transcription factor (e.g., PVX\_083040). ATATTTH is similar to the  
428 binding motif for *Pf*-AP2-L (AATTTCC), a transcription factor that is important for liver  
429 stage development in *P. berghei* [60]. In contrast to AP2-G, *Pv*-AP2-L (PVX\_081180) is in  
430 the top 10% of transcription and expression in *P. vivax* sporozoites and enriched relative to  
431 blood-stages. In *P. vivax* sporozoites, the ATATTTH motif is associated with a number of  
432 highly transcribed genes, including *lisp1* and *uis2-4*, known to be regulated by AP2-L in *P.*  
433 *berghei* [60] as well as many of the most highly transcribed, H3K9ac marked genes, including  
434 two *etramps* (PVX\_086815 and PVX\_088870), several RNA-binding proteins, including  
435 *Puf2*, *ddx5* and a dead-box helicase (PVX\_123240), as well as one of the putative *bax1*  
436 inhibitors (PVX\_101315). Interestingly, a number of highly transcribed and translationally  
437 repressed genes associated with the ATATTTH motif, including *uis4*, *siap2* and *pv1*, are not  
438 stably marked by H3K9ac in all replicates (i.e., there is significant variation in the placement  
439 of the H3K9ac peak or their presence/absence among replicates for these genes). It may be  
440 that additional histone modifications, for example H3K27me or H2 or H4 modifications, are  
441 involved in regulating transcription of these genes. Certainly H2A.Z, which is present in *P.*



442 *falciparum*, and controls temperature responses in plants [61] is intriguing as a potential mark  
443 regulating sporozoite fate in *P. vivax* considering the association between hypnozoite  
444 activation rate and climate [11].

445

## 446 **Conclusions**

447 We provide the first comprehensive study of the transcriptome, proteome and epigenome of  
448 infectious *Plasmodium vivax* sporozoites and the only study to integrate ‘omics investigation  
449 of the sporozoite of any *Plasmodium* species. These data support the proposal that the  
450 sporozoite is a highly-programmed stage that is primed for invasion of and development in  
451 the host hepatocyte. Translational repression clearly plays a major role in shaping this stage,  
452 with many of the genes proposed here as being under translational repression are involved in  
453 hepatocyte infection and early liver-stage development. We highlight a major role for RNA-  
454 binding proteins, including PUF2, ALBA2/4 and, intriguingly, ‘Homologue of Musashi’  
455 (HoMu). Noting that HoMu uses translational repression to regulate, in *Drosophila*, stem cell,  
456 and, in *Plasmodium*, gametocyte differentiation, it is intriguing to contemplate its potential  
457 role in setting liver-stage developmental fate. Identifying the sporozoite transcripts regulated  
458 by HoMu and other RNA binding proteins should be a key priority. As should in-depth  
459 comparative analysis using similar approaches of differences between/among relapsing and  
460 non-relapsing *Plasmodium* species, as well as, *P. vivax* field isolates with distinct, hypnozoite  
461 phenotypes. Our study provides a key foundation for understanding the early stages of  
462 hepatocyte infection and the developmental switch between liver trophozoite and hypnozoite  
463 formation. Importantly, it is a major first step in rationally prioritizing targets underpinning  
464 liver-stage differentiation for functional evaluation in humanized mouse and simian models  
465 for relapsing *Plasmodium* species and identifying novel avenues to understand and eradicate  
466 liver-stage infections.

467

## 468 **Methods**

### 469 **Material collection, isolation and preparation**

470 Nine field isolates (PvSpz-Thai 1 to 9), representing symptomatic blood-stage malaria  
471 infections were collected as venous blood (20 mL) from patients presenting at malaria clinics  
472 in Tak and Ubon Ratchatani provinces in Thailand. Each isolate was used to establish,  
473 infections in *Anopheles dirus* colonized at Mahidol University (Bangkok) by membrane  
474 feeding [13], after 14-16 days post blood feeding, ~3-15 million sporozoites were harvested  
475 per field isolate from the salivary glands of up to 1,000 of these mosquitoes as per [62] and  
476 shipped in preservative (trizol (RNA/DNA) or 1% paraformaldehyde (DNA for ChiP-seq)) to  
477 the Walter and Eliza Hall Institute (WEHI).

478

### 479 **Transcriptomics sequencing and differential analysis**

480 Upon arrival at WEHI, messenger RNAs were purified from an aliquot (~0.5-1 million  
481 sporozoites) of each *P. vivax* field isolate as per [29] and subjected to RNA-seq on Illumina  
482 NextSeq using TruSeq library construction chemistry as per the manufacturer’s instructions.  
483 Raw reads for each RNA-seq replicate are available through the Sequence Read Archive  
484 (XXX-XXX). Sequencing adaptors were removed and low quality reads trimmed and filtered  
485 using Trimmomatic v. 0.36 [63]. To remove host contaminants, processed reads were aligned,  
486 as single-end reads, to the *Anopheles dirus* wrari2 genome (VectorBase version W1) using  
487 Bowtie2[64] (--very-sensitive preset). All non-host reads were then aligned to the manually  
488 curated transcripts of the *P. vivax* P01 genome  
489 (<http://www.genedb.org/Homepage/PvivaxP01>) using RSEM [65] (pertinent settings: --  
490 bowtie2 --bowtie2-sensitivity-level very\_sensitive --calc-ci --ci-memory 10240 --estimate-  
491 rspd --paired-end). Transcript abundance for each gene in each replicate was calculated by  
492 RSEM as raw count, posterior mean estimate expected counts (pme-EC) and transcripts per  
493 million (TPM).

494 Transcriptional abundance in *P. vivax* sporozoites was compared qualitatively (by  
495 ranked abundance) with previously published microarray data for *P. vivax* salivary-gland  
496 sporozoites [23]. As a further quality control, these RNA-seq data were compared also with

497 previously published microarray data for *P. falciparum* salivary-gland sporozoites [26], as  
498 well as RNA-seq data from salivary-gland sporozoites generated here for *P. falciparum*  
499 (single replicate generated from *P. falciparum* 3D7 lab cultures isolated from *Anopheles*  
500 *stephensi* and processed as above) and previously published for *P. yoelii* [25]. RNA-seq data  
501 from these additional *Plasmodium* species were (re)analysed from raw reads and  
502 transcriptional abundance for each species was determined (raw counts and pme-EC and TPM  
503 data) as described above using gene models current as of 04-10-2016 (PlasmoDB release  
504 v29). Interspecific transcriptional behaviour was qualitatively compared by relative ranked  
505 abundance in each species using TPM data for single copy orthologs (SCOs; defined in  
506 PlasmoDB) only, shared between *P. vivax* and *P. falciparum* or shared among *P. vivax*, *P.*  
507 *falciparum* and *P. yoelii*.

508 To define sporozoite-enriched transcripts, we remapped raw reads representing early  
509 (18-24 hours post-infection (HPI)), mid (30-40 HPI) and late (42-46 HPI) *P. vivax* blood-  
510 stage infections recently published by Zhu *et al* [29] to the *P. vivax* P01 transcripts using  
511 RSEM as above. All replicate data was assessed for mapping metrics, transcript saturation  
512 and other standard QC metrics using QualiMap v 2.1.3 [66]. Differential transcription  
513 between *P. vivax* salivary-gland sporozoites and mixed blood-stages [29] was assessed using  
514 pme-EC data in EdgeR [67] (differential transcription cut-off:  $\geq 2$ -fold change in counts per  
515 million (CPM) and a False Discovery Rate (FDR)  $\leq 0.05$ ). Pearson Chi squared tests were  
516 used to detect over-represented Pfam domains and Gene Ontology (GO) terms among  
517 differentially transcribed genes in sporozoites (Bonferroni-corrected  $p < 0.05$ ), based on gene  
518 annotations in PlasmoDB (release v29).

519

## 520 **Proteomic sequencing and quantitative analysis**

521 Aliquots of  $\sim 10^7$  salivary-gland sporozoites were generated from PvSpz-Thai1 and PvSpz-  
522 Thai6 isolates, purified on an Accudenz gradient per [62] and shipped on dry ice (protein) to  
523 the Center for Infectious Disease Research (CIDR). These cells were lysed in 2x Sample  
524 Buffer and their proteins separated by SDS-PAGE per [40]. For the whole proteome analysis,  
525 each gel was run out 52 mm and cut into 27-29 fractions using a grid cutter (Gel Company,  
526 San Francisco, CA). Pooled peptides in each gel fraction were reduced in dithiothreitol /  
527 ammonium bicarbonate, and digested for 4.5 hours at 36 °C in 6.25 ng/mL trypsin under  
528 vortex at 700 RPM. The supernatant was recovered and peptides were extracted by incubating  
529 the gel in 2% (v/v) acetonitrile/1% (v/v) formic acid. Supernatant after three extractions was  
530 combined with the digest supernatant, evaporated to dryness in a rotary vacuum, and  
531 reconstituted in HPLC loading buffer consisting of 2% (v/v) acetonitrile/0.2% (v/v)  
532 trifluoroacetic acid. Nanoflow liquid chromatography (nanoLC) was performed using an  
533 Agilent 1100 nano pump with electronically controlled split flow or a Proxeon Easy nLC.  
534 Peptides were separated on a column with an integrated fritted tip (360  $\mu\text{m}$  outer diameter  
535 (O.D.), 75  $\mu\text{m}$  inner diameter (I.D.), 15  $\mu\text{m}$  I.D. tip; New Objective) packed in-house with a  
536 20 cm bed of C18 (Dr. Maisch ReproSil-Pur C18-AQ, 120 Å, 3  $\mu\text{m}$ ; Ammerbuch-Entringen,  
537 Germany). Tandem mass spectrometry (MS/MS) was performed with an LTQ Velos Pro-  
538 Orbitrap Elite (Thermo Fisher Scientific). Two nanoLC-MS technical replicates were  
539 performed for each fraction, with roughly half the available sample injected for each  
540 replicate. The mass spectrometry data generated for this manuscript, along with the search  
541 parameters, analysis parameters and protein databases can be downloaded from PeptideAtlas  
542 ([www.peptideatlas.org](http://www.peptideatlas.org)) using the identifier #####.

543 Mass spectrometer output files were converted to .mZML format using MSConvert  
544 version 2.2.0 (whole proteome data) or 3.0.5533 (surface-labeled data) [68] and searched with  
545 X!Tandem [69] version 2013.06.15.1 JACKHAMMER and Comet version 2015.02 rev.0.[70]  
546 MS/MS data were analyzed using the Trans-Proteomic Pipeline[71] version 4.8.0 PHILAE.  
547 Peptide spectrum matches (PSM) generated by each search engine were analyzed separately  
548 with PeptideProphet [72] and combined in iProphet.[73] Protein identifications were inferred  
549 with ProteinProphet [74]. In the case that multiple proteins were inferred at equal confidence  
550 by a set of peptides, the inference was counted as a single identification and all relevant  
551 protein IDs were listed. Only proteins with ProteinProphet probabilities corresponding to a

552 model-estimated false discovery rate (FDR) less than 1.0 % were reported. Spectra were  
553 searched against a protein sequence database comprised of *P. vivax* P01 (version 29,  
554 [www.plasmodb.org](http://www.plasmodb.org)), *An. stephensi* SDA 500 (version 1.3, [www.vectorbase.org](http://www.vectorbase.org)), and a  
555 modified version of the common Repository of Adventitious Proteins (version 2012.01.01,  
556 [www.thegpm.org/cRAP](http://www.thegpm.org/cRAP)) with the Sigma Universal Standard Proteins removed and the LC  
557 calibration standard peptide [Glu-1] fibrinopeptide B appended. Label-free proteomics  
558 methods based on spectral counts (SpC) were used to identify proteins that were significantly  
559 more abundant in labeled samples compared to unlabeled controls. The SpC for a given  
560 protein in a given biological replicate was taken as the number of PSM used by  
561 ProteinProphet to make the protein inference. All SpC values were increased by one in order  
562 to give all proteins non-zero SpC values for log-transformation [75]. The spectral abundance  
563 factor (SAF) for a given protein was calculated as the quotient of the SpC and the protein's  
564 length and natural log-transformed to  $\ln(\text{SAF})$  [76]. For a more detailed description of the  
565 proteome data collection process and analysis please refer to manuscript by Swearingen *et al*  
566 (*submitted*).

567 To identify genes likely under translational repression in the *P. vivax* sporozoite, we  
568 examined these data for genes that were highly transcribed (top 10 percentile) but for which  
569 we could find no evidence of protein expression in any sporozoite replicate. In addition, we  
570 conducted abundance ranked comparisons between the mean transcriptional abundance of  
571 each *P. vivax* gene in sporozoites (see above) and the mean quantitative abundance of its  
572 protein in our expressional data. Genes were sorted on the differential between their relative  
573 transcription and relative expression ranking to identify highly transcribed genes with  
574 substantially lower expression relative to their transcriptional abundance.

575

#### 576 **Salivary-gland sporozoite and liver-stage immunofluorescence assays (IFAs)**

577 IFAs were performed as per [13]. Liver stages were obtained from 10 $\mu$ m formalin fixed  
578 paraffin embedded day 7 liver stages generated previously [13] from FRG knockout huHep  
579 mice; [13] these were deparaffinized prior to staining. Fresh salivary-gland sporozoites were  
580 fixed in acetone per [13]. All cells were incubated twice for 3 minutes in Xylene, then 100%  
581 Ethanol, and finally once for 3 minutes each in 95%, 70%, and 50% Ethanol. The cells were  
582 rinsed in DI water and permeabilized immediately in 1XTBS, containing Triton X-100 and  
583 30% hydrogen peroxide. The cells were blocked in 5% milk in 1XTBS. The hepatocytes were  
584 stained overnight with a rabbit polyclonal LISP1 antibody (A), a rabbit polyclonal UIS4  
585 antibody (B), and a rabbit polyclonal BIP antibody (C) in blocking buffer. The cells were  
586 washed with 1XTBS and the primary antibodies were detected with goat anti-rabbit Alexa  
587 Fluor 488 antibody (Life Technologies). The cells were washed in 1XTBS. The hepatocytes  
588 were rinsed in KMNO<sub>4</sub> and washed in 1XTBS. The cells were incubated in DAPI for 5  
589 minutes.

590

#### 591 **Histone ChIP sequencing and analysis**

592 Aliquots of 2 – 6 million freshly isolated sporozoites were fixed with 1% paraformaldehyde  
593 for 10 min at 37°C and the reaction subsequently quenched by adding glycine to a final  
594 concentration of 125 mM. After three washes with PBS, sporozoite pellets were stored at -  
595 80°C and shipped to Australia. Nuclei were released from the sporozoites by dounce  
596 homogenization in lysis buffer (10 mM Hepes pH 7.9, 10 mM KCl, 0.1 mM EDTA, 0.1 mM  
597 EDTA, 1 mM DTT, 1x EDTA-free protease inhibitor cocktail (Roche), 0.25% NP40). Nuclei  
598 were pelleted by centrifugation at 21,000 g for 10 min at 4°C and resuspended in SDS lysis  
599 buffer (1% SDS, 10 mM EDTA, 50 mM Tris pH 8.1, 1x EDTA-free protease inhibitor  
600 cocktail). Chromatin was sheared into 200–1000 bp fragments by sonication for 16 cycles in  
601 30 sec intervals (on/off, high setting) using a Bioruptor (Diagenode) and diluted 1:10 in ChIP  
602 dilution buffer (0.01% SDS, 1.1% Triton X-100, 1.2 mM EDTA, 16.7 mM Tris pH 8.1, 150  
603 mM NaCl). Chromatin was precleared for 1 hour with protein A/G sepharose (4FastFlow, GE  
604 Healthcare) equilibrated in 0.1% BSA in ChIP dilution buffer. Chromatin from 3 x 10<sup>5</sup> nuclei  
605 was taken aside as input material. Chromatin from approximately 3 x 10<sup>6</sup> sporozoite nuclei  
606 was used for each ChIP. ChIP was carried out over night at 4°C with 5  $\mu$ g of antibody

607 (H3K9me3 (Active Motif), H3K4me3 (Abcam), H3K9ac (Upstate), H4K16ac (Abcam)) and  
608 10  $\mu$ l each of equilibrated protein A and G sepharose beads (4FastFlow, GE Healthcare).  
609 After washes in low-salt, high-salt, LiCl, and TE buffers (EZ-ChIP Kit, Millipore),  
610 precipitated complexes were eluted in 1% SDS, 0.1 M NaHCO<sub>3</sub>. Cross-linking of the immune  
611 complexes and input material was reversed for 6 hours at 45°C after addition of 500 mM  
612 NaCl and 20  $\mu$ g/ml of proteinase K (NEB). DNA was purified using the MinElute® PCR  
613 purification kit (Qiagen) and paired-end sequenced on Illumina NextSeq using TruSeq library  
614 construction chemistry as per the manufacturer's instructions. Raw reads for each ChIP-seq  
615 replicate are available through the Sequence Read Archive (XXX-XXX).

616 Fastq files were checked for quality using fastqc  
617 (<http://www.bioinformatics.babraham.ac.uk/projects/fastqc/>) and adapter sequences were  
618 trimmed using cutadapt [77]. Paired end reads were mapped to the *P. vivax* P01 strain  
619 genome annotation using Bowtie2 [64]. The alignment files were converted to Bam format,  
620 sorted and indexed using Samtools [78]. ChIP peaks were called relative to input using  
621 MACS2[79] in paired end mode with a q value less than or equal to 0.01. Peaks and peak  
622 summits were converted to sorted BED files. Bedtools intersect[80] was used to identify  
623 genes that intersected H3K9me3 peaks and Bedtools closest was used to identify genes that  
624 were closest to and downstream of H3K9ac and H3K4me3 peak summits.

625

### 626 **Sequence motif analysis**

627 Conserved sequence motifs were identified using the program DREME [81]. Only genes in  
628 the top decile of transcription showing no evidence of protein expression in multiple salivary-  
629 gland sporozoite replicates were considered as putatively translationally repressed (n = 170).  
630 We queried coding regions and regions upstream of the transcriptional start site (TSS) for  
631 each gene, defined by Zhu *et al* [29] and/or predicted here from all RNA-seq data using the  
632 Tuxedo suite [82], for enriched sequence motifs in comparison to 170 genes found to be in  
633 the top decile of both transcriptional and expressional abundance in the same sporozoite  
634 replicates. In searching for motifs associated with highly transcribed genes with stable  
635 H3K9ac marks within 1kb of the TSS (or up to the 3' end of the next gene upstream), we  
636 compared H3K9ac marked genes in the top decile of transcription to the same number of  
637 H3K9ac marked genes in the bottom decile of transcription. In both instances, an e-value  
638 threshold of 0.05 was considered the minimum threshold for statistical significance.

639

640 **Author contributions:** Study design and development: Ivo Muller<sup>1,2,3</sup> (IM), Aaron R. Jex<sup>1,3,4</sup>  
641 (AJ), Stefan H. I. Kappe<sup>5</sup> (SK) and Sebastian A. Mikolajczak<sup>5</sup> (SM); Parasite collection and  
642 sporozoite production and purification: Jetsumon Sattabongkot<sup>7</sup> (JSP), Rapatbhorn  
643 Patrapuvich<sup>6</sup> (RP), SK, SM, Scott Lindner<sup>8</sup> (SL) and Erika L. Flannery<sup>5</sup> (EF); DNA/RNA  
644 isolation and sequence library preparation: Cristian Koepfli<sup>1</sup> (CK) and EF; Transcriptomics  
645 analysis: AJ, Brendan Ansell<sup>4</sup> (BA) and Anita Lerch<sup>1</sup> (AL); Proteomics analysis: Kristian  
646 Swearingen<sup>5</sup> (KS), Robert Moritz (RM)<sup>9</sup> SL, SM and EF; ChIP-seq preparation and analyses:  
647 Michaela Petter<sup>10</sup> (MP) and Michael Duffy<sup>10</sup> (MD); Immunofluorescence assays: Vorada  
648 Chuenchob<sup>5</sup>; Data integration and interpretation: AJ, IM, EF, SM and SK; Manuscript  
649 preparation: AJ, IM, SM, SK, SL, and EF.

650

651 **Author affiliations:** 1. Population Health and Immunity Division, The Walter and Eliza Hall  
652 Institute for Medical Research, 1G Royal Parade, Parkville, Victoria, 3052, Australia; 2.  
653 Malaria: Parasites & Hosts Unit, Institut Pasteur, 28 Rue de Dr. Roux, 75015, Paris, France;  
654 3. Department of Medical Biology, The University of Melbourne, Victoria, 3010, Australia;  
655 4. Faculty of Veterinary and Agricultural Sciences, The University of Melbourne, Corner of  
656 Park and Flemington Road, Parkville, Victoria, 3010, Australia; 5. Center for Infectious  
657 Disease Research, 307 Westlake Avenue North, Suite 500, Seattle, WA 98109, USA; 6.  
658 Department of Global Health, University of Washington, Seattle, WA 98195, USA; 7.  
659 Mahidol Vivax Research Center, Faculty of Tropical Medicine, Mahidol University, Bangkok  
660 10400, Thailand; 8. Department of Biochemistry and Molecular Biology, Center for Malaria  
661 Research, Pennsylvania State University, University Park, PA 16802, USA. 9. Institute for

662 Systems Biology, Seattle, WA, 98109, USA. 10. Department of Medicine Royal Melbourne  
663 Hospital, The Peter Doherty Institute, The University of Melbourne, 792 Elizabeth Street,  
664 Melbourne, Victoria 3000, Australia

665

666 **Acknowledgements:** The authors acknowledge funding from the National Health and  
667 Medical Research Council (NHMRC, APP1021544, 1043345, & 1092789), the Australian  
668 Research Council (ARC), the Victorian State Government Operational Infrastructure Support  
669 and Australian Government National Health and Medical Research Council Independent  
670 Research Institute Infrastructure Support Scheme, the Ian Potter Foundation, the National  
671 Institute of Health, the Bill and Melinda Gates Foundation, the US Department of Defense  
672 (W81XWH-15-1-0249) and the Office of the Assistant Secretary of Defence for Health  
673 Affairs through the Peer Reviewed Medical Research Program (PRMRP).

674

675 **Competing Interests:** The authors declare that no author of this manuscript has a competing  
676 financial or non-financial interest related to this work.

677

678

679

## References

680

1. Organization WH: World Malaria Report 2015. WHO, Geneva. 2015.

681

2. Feachem RG, Phillips AA, Hwang J, Cotter C, Wielgosz B, Greenwood BM, et al:  
682 Shrinking the malaria map: progress and prospects. *Lancet*.  
683 2010;376(9752):1566-78.

684

3. Price RN, Douglas NM, Anstey NM: New developments in *Plasmodium vivax*  
685 malaria: severe disease and the rise of chloroquine resistance. *Curr Opin Infect*  
686 *Dis*. 2009;22(5):430-5.

687

4. Baird KJ: Malaria caused by *Plasmodium vivax*: recurrent, difficult to treat,  
688 disabling, and threatening to life - averting the infectious bite preempts these  
689 hazards. *Pathogens Global Health*. 2013;107475-9.

690

5. Sattabongkot J, Tsuboi T, Zollner GE, Sirichaisinthop J, Cui L: *Plasmodium vivax*  
691 transmission: chances for control? *Trends Parasitol*. 2004;20(4):192-8.

692

6. Mueller I, Galinski MR, Baird JK, Carlton JM, Kochar DK, Alonso PL, et al: Key gaps  
693 in the knowledge of *Plasmodium vivax*, a neglected human malaria parasite.  
694 *Lancet Infect Dis*. 2009;9(9):555-66.

695

7. Lindner SE, Miller JL, Kappe SH: Malaria parasite pre-erythrocytic infection:  
696 preparation meets opportunity. *Cell Microbiol*. 2012;14(3):316-24.

697

8. Mota MM, Pradel G, Vanderberg JP, Hafalla JC, Frevert U, Nussenzweig RS, et al:  
698 Migration of *Plasmodium* sporozoites through cells before infection. *Science*.  
699 2001;291(5501):141-4.

700

9. Shin SC, Vanderberg JP, Terzakis JA: Direct infection of hepatocytes by  
701 sporozoites of *Plasmodium berghei*. *J Protozool*. 1982;29(3):448-54.

702

10. Lysenko AJ, Beljaev A, Rybalka V: Population studies of *Plasmodium vivax*: 1. The  
703 theory of polymorphism of sporozoites and epidemiological phenomena of  
704 tertian malaria. *Bulletin WHO*. 1977;55(5):541.

705

11. White NJ: Determinants of relapse periodicity in *Plasmodium vivax* malaria.  
706 *Malar J*. 2011;10297.

707

12. Price RN, Tjitra E, Guerra CA, Yeung S, White NJ, Anstey NM: Vivax malaria:  
708 neglected and not benign. *Amer J Trop Med Hyg*. 2007;77(6 Suppl):79-87.

709

13. Mikolajczak SA, Vaughan AM, Kangwanrangsan N, Roobsoong W, Fishbaugher M,  
710 Yimamnuaychok N, et al: *Plasmodium vivax* liver stage development and  
711 hypnozoite persistence in human liver-chimeric mice. *Cell Host Microbe*.  
712 2015;17(4):526-35.

713

14. Mueller A-K, Camargo N, Kaiser K, Andorfer C, Frevert U, Matuschewski K, et al:  
714 *Plasmodium* liver stage developmental arrest by depletion of a protein at the  
715 parasite-host interface. *Proc Natl Acad Sci U S A*. 2005;102(8):3022-7.

- 716 15. Silvie O, Briquet S, Muller K, Manzoni G, Matuschewski K: Post-transcriptional  
717 silencing of UIS4 in *Plasmodium berghei* sporozoites is important for host switch.  
718 Mol Microbiol. 2014;91(6):1200-13.
- 719 16. Mackellar DC, O'Neill MT, Aly AS, Sacci JB, Jr., Cowman AF, Kappe SH:  
720 *Plasmodium falciparum* PF10\_0164 (ETRAP10.3) is an essential  
721 parasitophorous vacuole and exported protein in blood stages. Eukaryot Cell.  
722 2010;9(5):784-94.
- 723 17. Dembele L, Franetich JF, Lorthiois A, Gego A, Zeeman AM, Kocken CH, et al:  
724 Persistence and activation of malaria hypnozoites in long-term primary  
725 hepatocyte cultures. Nat Med. 2014;20(3):307-12.
- 726 18. Malmquist NA, Moss TA, Mecheri S, Scherf A, Fuchter MJ: Small-molecule histone  
727 methyltransferase inhibitors display rapid antimalarial activity against all blood  
728 stage forms in *Plasmodium falciparum*. Proc Natl Acad Sci U S A.  
729 2012;109(41):16708-13.
- 730 19. Josling GA, Llinas M: Sexual development in *Plasmodium* parasites: knowing  
731 when it's time to commit. Nat Rev Microbiol. 2015;13(9):573-87.
- 732 20. White MT, Karl S, Battle KE, Hay SI, Mueller I, Ghani AC: Modelling the  
733 contribution of the hypnozoite reservoir to *Plasmodium vivax* transmission. Elife.  
734 2014;3.
- 735 21. Roobsoong W, Tharinjaroen CS, Rachaphaew N, Chobson P, Schofield L, Cui L, et  
736 al: Improvement of culture conditions for long-term in vitro culture of  
737 *Plasmodium vivax*. Malaria J. 2015;14(1):1.
- 738 22. Cubi R, Vembar SS, Biton A, Franetich JF, Bordessoulles M, Sossau D, et al: Laser  
739 capture microdissection enables transcriptomic analysis of dividing and  
740 quiescent liver stages of *Plasmodium* relapsing species. Cell Microbiol. 2017.
- 741 23. Westenberger SJ, McClean CM, Chattopadhyay R, Dharia NV, Carlton JM,  
742 Barnwell JW, et al: A systems-based analysis of *Plasmodium vivax* lifecycle  
743 transcription from human to mosquito. PLoS Negl Trop Dis. 2010;4(4):e653.
- 744 24. Gomez-Diaz E, Yerbanga RS, Lefevre T, Cohuet A, Rowley MJ, Ouedraogo JB, et al:  
745 Epigenetic regulation of *Plasmodium falciparum* clonally variant gene expression  
746 during development in *Anopheles gambiae*. Sci Rep. 2017;740655.
- 747 25. Lindner SE, Mikolajczak SA, Vaughan AM, Moon W, Joyce BR, Sullivan WJ, Jr., et  
748 al: Perturbations of *Plasmodium* Puf2 expression and RNA-seq of Puf2-deficient  
749 sporozoites reveal a critical role in maintaining RNA homeostasis and parasite  
750 transmissibility. Cell Microbiol. 2013;15(7):1266-83.
- 751 26. Le Roch KG, Johnson JR, Florens L, Zhou Y, Santrosyan A, Grainger M, et al: Global  
752 analysis of transcript and protein levels across the *Plasmodium falciparum* life  
753 cycle. Genome Res. 2004;14(11):2308-18.
- 754 27. Mikolajczak SA, Silva-Rivera H, Peng X, Tarun AS, Camargo N, Jacobs-Lorena V, et  
755 al: Distinct malaria parasite sporozoites reveal transcriptional changes that  
756 cause differential tissue infection competence in the mosquito vector and  
757 mammalian host. Mol Cell Biol. 2008;28(20):6196-207.
- 758 28. Carlton JM, Adams JH, Silva JC, Bidwell SL, Lorenzi H, Caler E, et al: Comparative  
759 genomics of the neglected human malaria parasite *Plasmodium vivax*. Nature.  
760 2008;455(7214):757-63.
- 761 29. Zhu L, Mok S, Imwong M, Jaidee A, Russell B, Nosten F, et al: New insights into  
762 the *Plasmodium vivax* transcriptome using RNA-Seq. Sci Rep. 2016;620498.
- 763 30. Kramer S: RNA in development: how ribonucleoprotein granules regulate the life  
764 cycles of pathogenic protozoa. WIR: RNA. 2014;5(2):263-84.
- 765 31. Tucker RP: The thrombospondin type 1 repeat superfamily. Int J Biochem Cell  
766 Biol. 2004;36(6):969-74.
- 767 32. Ntumngia FB, Bouyou-Akotet MK, Uhlemann AC, Mordmuller B, Kremsner PG,  
768 Kun JF: Characterisation of a tryptophan-rich *Plasmodium falciparum* antigen  
769 associated with merozoites. Mol Biochem Parasitol. 2004;137(2):349-53.

- 770 33. Gubbels MJ, Vaishnava S, Boot N, Dubremetz JF, Striepen B: A MORN-repeat  
771 protein is a dynamic component of the *Toxoplasma gondii* cell division  
772 apparatus. *J Cell Sci.* 2006;119(Pt 11):2236-45.
- 773 34. Aly AS, Lindner SE, MacKellar DC, Peng X, Kappe SH: SAP1 is a critical post-  
774 transcriptional regulator of infectivity in malaria parasite sporozoite stages. *Mol*  
775 *Microbiol.* 2011;79(4):929-39.
- 776 35. Okano H, Imai T, Okabe M: Musashi: a translational regulator of cell fate. *J Cell*  
777 *Sci.* 2002;115(7):1355-9.
- 778 36. Cui L, Lindner S, Miao J: Translational regulation during stage transitions in  
779 malaria parasites. *Annals N Y Acad Sci.* 2015;1342(1):1-9.
- 780 37. Lasko P: Gene regulation at the RNA layer: RNA binding proteins in intercellular  
781 signaling networks. *Sci STKE.* 2003;179RE6.
- 782 38. Guerreiro A, Deligianni E, Santos JM, Silva PA, Louis C, Pain A, et al: Genome-wide  
783 RIP-Chip analysis of translational repressor-bound mRNAs in the *Plasmodium*  
784 gametocyte. *Genome Biol.* 2014;15(11):493.
- 785 39. Kappe SH, Buscaglia CA, Bergman LW, Coppens I, Nussenzweig V: Apicomplexan  
786 gliding motility and host cell invasion: overhauling the motor model. *Trends in*  
787 *parasitology.* 2004;20(1):13-6.
- 788 40. Lindner SE, Swearingen KE, Harupa A, Vaughan AM, Sinnis P, Moritz RL, et al:  
789 Total and putative surface proteomics of malaria parasite salivary gland  
790 sporozoites. *Mol Cell Proteomics.* 2013;12(5):1127-43.
- 791 41. Silvie O, Briquet S, Müller K, Manzoni G, Matuschewski K: Post-transcriptional  
792 silencing of UIS4 in *Plasmodium berghei* sporozoites is important for host switch.  
793 *Molecular microbiology.* 2014;91(6):1200-13.
- 794 42. Kelley KD, Miller KR, Todd A, Kelley AR, Tuttle R, Berberich SJ: YPEL3, a p53-  
795 regulated gene that induces cellular senescence. *Cancer Res.* 2010;70(9):3566-  
796 75.
- 797 43. Tuttle R, Simon M, Hitch DC, Maiorano JN, Hellan M, Ouellette J, et al:  
798 Senescence-associated gene YPEL3 is downregulated in human colon tumors.  
799 *Ann Surg Oncol.* 2011;18(6):1791-6.
- 800 44. Struck NS, de Souza Dias S, Langer C, Marti M, Pearce JA, Cowman AF, et al: Re-  
801 defining the Golgi complex in *Plasmodium falciparum* using the novel Golgi  
802 marker PfGRASP. *J Cell Sci.* 2005;118(Pt 23):5603-13.
- 803 45. Graewe S, Stanway RR, Rennenberg A, Heussler VT: Chronicle of a death  
804 foretold: *Plasmodium* liver stage parasites decide on the fate of the host cell.  
805 *FEMS Microbiol Rev.* 2012;36(1):111-30.
- 806 46. Bruchhaus I, Roeder T, Rennenberg A, Heussler VT: Protozoan parasites:  
807 programmed cell death as a mechanism of parasitism. *Trends Parasitol.*  
808 2007;23(8):376-83.
- 809 47. Albuquerque SS, Carret C, Grosso AR, Tarun AS, Peng X, Kappe SH, et al: Host cell  
810 transcriptional profiling during malaria liver stage infection reveals a  
811 coordinated and sequential set of biological events. *BMC genomics.*  
812 2009;10(1):1.
- 813 48. Kaushansky A, Metzger PG, Douglass AN, Mikolajczak SA, Lakshmanan V, Kain  
814 HS, et al: Malaria parasite liver stages render host hepatocytes susceptible to  
815 mitochondria-initiated apoptosis. *Cell Death Dis.* 2013;4e762.
- 816 49. Liu M, Miao J, Liu T, Sullivan WJ, Cui L, Chen X: Characterization of TgPuf1, a  
817 member of the Puf family RNA-binding proteins from *Toxoplasma gondii*.  
818 *Parasites & vectors.* 2014;7(1):1.
- 819 50. Miao J, Fan Q, Parker D, Li X, Li J, Cui L: Puf mediates translation repression of  
820 transmission-blocking vaccine candidates in malaria parasites. *PLoS Pathog.*  
821 2013;9(4):e1003268.
- 822 51. Yuda M, Iwanaga S, Shigenobu S, Kato T, Kaneko I: Transcription factor AP2-Sp  
823 and its target genes in malarial sporozoites. *Mol Microbiol.* 2010;75(4):854-63.

- 824 52. Lopez-Rubio J-J, Mancio-Silva L, Scherf A: Genome-wide analysis of  
825 heterochromatin associates clonally variant gene regulation with perinuclear  
826 repressive centers in malaria parasites. *Cell Host Microbe*. 2009;5(2):179-90.
- 827 53. Duffy MF, Selvarajah SA, Josling GA, Petter M: Epigenetic regulation of the  
828 *Plasmodium falciparum* genome. *Brief Funct Genomics*. 2014;13(3):203-16.
- 829 54. Cui L, Miao J, Furuya T, Li X, Su XZ, Cui L: PfGCN5-mediated histone H3  
830 acetylation plays a key role in gene expression in *Plasmodium falciparum*.  
831 *Eukaryot Cell*. 2007;6(7):1219-27.
- 832 55. Guizetti J, Scherf A: Silence, activate, poise and switch! Mechanisms of antigenic  
833 variation in *Plasmodium falciparum*. *Cell Microbiol*. 2013;15(5):718-26.
- 834 56. Rovira-Graells N, Gupta AP, Planet E, Crowley VM, Mok S, de Pouplana LR, et al:  
835 Transcriptional variation in the malaria parasite *Plasmodium falciparum*.  
836 *Genome Res*. 2012;22(5):925-38.
- 837 57. De Silva EK, Gehrke AR, Olszewski K, León I, Chahal JS, Bulyk ML, et al: Specific  
838 DNA-binding by apicomplexan AP2 transcription factors. *Proc Natl Acad Sci U S*  
839 *A*. 2008;105(24):8393-8.
- 840 58. Painter HJ, Campbell TL, Llinás M: The Apicomplexan AP2 family: integral factors  
841 regulating *Plasmodium* development. *Mol Biochem Parasitol*. 2011;176(1):1-7.
- 842 59. Kafsack BF, Rovira-Graells N, Clark TG, Bancells C, Crowley VM, Campino SG, et  
843 al: A transcriptional switch underlies commitment to sexual development in  
844 human malaria parasites. *Nature*. 2014;507(7491):248.
- 845 60. Iwanaga S, Kaneko I, Kato T, Yuda M: Identification of an AP2-family protein that  
846 is critical for malaria liver stage development. *PLoS One*. 2012;7(11):e47557.
- 847 61. Boden SA, Kavanova M, Finnegan EJ, Wigge PA: Thermal stress effects on grain  
848 yield in *Brachypodium distachyon* occur via H2A.Z-nucleosomes. *Genome Biol*.  
849 2013;14(6):R65.
- 850 62. Kennedy M, Fishbaugher ME, Vaughan AM, Patrapuvich R, Boonhok R,  
851 Yimamnuaychok N, et al: A rapid and scalable density gradient purification  
852 method for *Plasmodium* sporozoites. *Malar J*. 2012;11:421.
- 853 63. Bolger AM, Lohse M, Usadel B: Trimmomatic: a flexible trimmer for Illumina  
854 sequence data. *Bioinformatics*. 2014;30(15):2114-20.
- 855 64. Langmead B, Salzberg SL: Fast gapped-read alignment with Bowtie 2. *Nat*  
856 *Methods*. 2012;9(4):357-9.
- 857 65. Li B, Dewey CN: RSEM: accurate transcript quantification from RNA-Seq data  
858 with or without a reference genome. *BMC Bioinformatics*. 2011;12(1):323.
- 859 66. Okonechnikov K, Conesa A, Garcia-Alcalde F: Qualimap 2: advanced multi-  
860 sample quality control for high-throughput sequencing data. *Bioinformatics*.  
861 2016;32(2):292-4.
- 862 67. Nikolayeva O, Robinson MD: edgeR for differential RNA-seq and ChIP-seq  
863 analysis: an application to stem cell biology. *Methods Mol Biol*. 2014;1150:45-79.
- 864 68. Kessner D, Chambers M, Burke R, Agus D, Mallick P: ProteoWizard: open source  
865 software for rapid proteomics tools development. *Bioinformatics*.  
866 2008;24(21):2534-6.
- 867 69. Craig R, Beavis RC: TANDEM: matching proteins with tandem mass spectra.  
868 *Bioinformatics*. 2004;20(9):1466-7.
- 869 70. Eng JK, Jahan TA, Hoopmann MR: Comet: an open-source MS/MS sequence  
870 database search tool. *Proteomics*. 2013;13(1):22-4.
- 871 71. Deutsch EW, Mendoza L, Shteynberg D, Slagel J, Sun Z, Moritz RL: Trans-  
872 Proteomic Pipeline, a standardized data processing pipeline for large-scale  
873 reproducible proteomics informatics. *Proteomics Clin Appl*. 2015;9(7-8):745-54.
- 874 72. Keller A, Nesvizhskii AI, Kolker E, Aebersold R: Empirical statistical model to  
875 estimate the accuracy of peptide identifications made by MS/MS and database  
876 search. *Anal Chem*. 2002;74(20):5383-92.



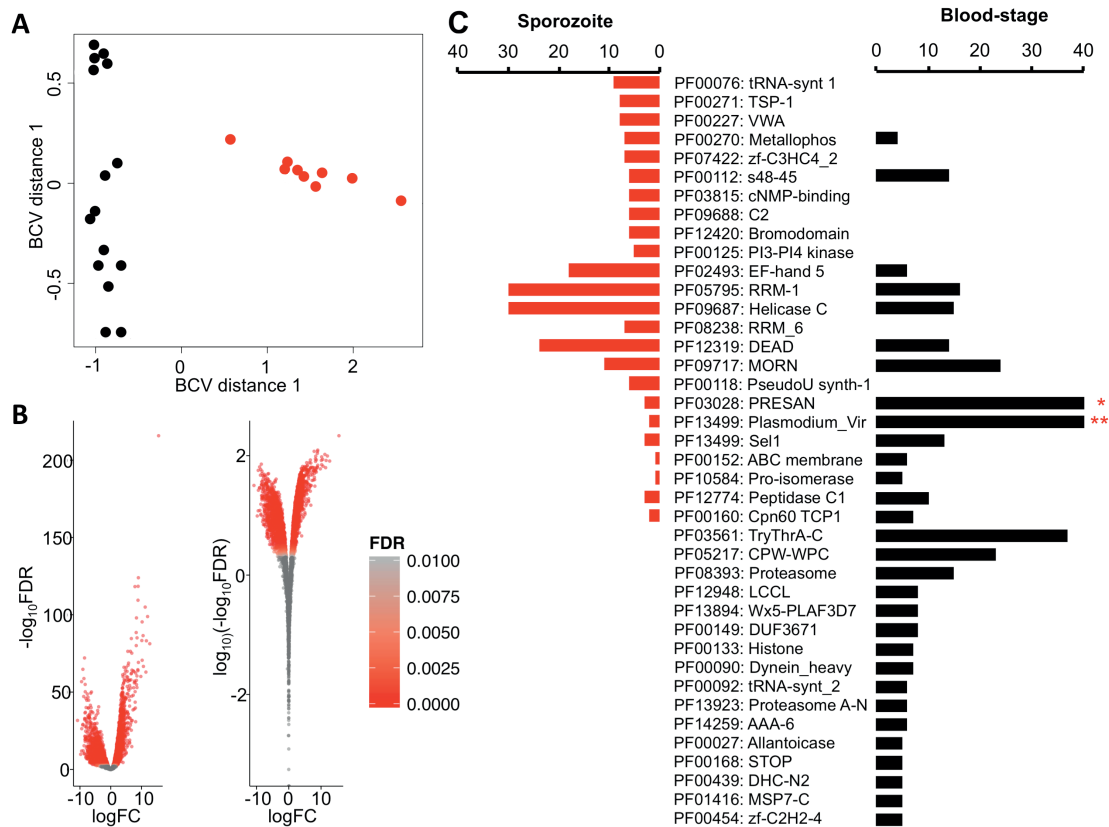
- 877 73. Shteynberg D, Deutsch EW, Lam H, Eng JK, Sun Z, Tasman N, et al: iProphet:  
878 multi-level integrative analysis of shotgun proteomic data improves peptide and  
879 protein identification rates and error estimates. *Mol Cell Proteomics*.  
880 2011;10(12):M111 007690.
- 881 74. Nesvizhskii AI, Keller A, Kolker E, Aebersold R: A statistical model for identifying  
882 proteins by tandem mass spectrometry. *Anal Chem*. 2003;75(17):4646-58.
- 883 75. Hendrickson EL, Xia Q, Wang T, Leigh JA, Hackett M: Comparison of spectral  
884 counting and metabolic stable isotope labeling for use with quantitative  
885 microbial proteomics. *Analyst*. 2006;131(12):1335-41.
- 886 76. Zybilov B, Mosley AL, Sardu ME, Coleman MK, Florens L, Washburn MP:  
887 Statistical analysis of membrane proteome expression changes in  
888 *Saccharomyces cerevisiae*. *J Proteome Res*. 2006;5(9):2339-47.
- 889 77. Martin M: Cutadapt removes adapter sequences from high-throughput  
890 sequencing reads. *EMBnet journal*. 2011;17(1):pp. 10-2.
- 891 78. Li H, Handsaker B, Wysoker A, Fennell T, Ruan J, Homer N, et al: The Sequence  
892 Alignment/Map format and SAMtools. *Bioinformatics*. 2009;25(16):2078-9.
- 893 79. Zhang Y, Liu T, Meyer CA, Eeckhoute J, Johnson DS, Bernstein BE, et al: Model-  
894 based analysis of ChIP-Seq (MACS). *Genome Biol*. 2008;9(9):R137.
- 895 80. Quinlan AR, Hall IM: BEDTools: a flexible suite of utilities for comparing genomic  
896 features. *Bioinformatics*. 2010;26(6):841-2.
- 897 81. Bailey TL: DREME: motif discovery in transcription factor ChIP-seq data.  
898 *Bioinformatics*. 2011;27(12):1653-9.
- 899 82. Trapnell C, Roberts A, Goff L, Pertea G, Kim D, Kelley DR, et al: Differential gene  
900 and transcript expression analysis of RNA-seq experiments with TopHat and  
901 Cufflinks. *Nat Protoc*. 2012;7(3):562-78.  
902  
903

904 **Figures**

905

906 **Fig. 1** Differential transcription between *Plasmodium vivax* salivary-gland sporozoites  
 907 and blood-stages. **a** BCV plot showing separation between blood-stage (black) and  
 908 salivary-gland sporozoite (red) biological replicates. **b** Volcano plot of distribution of  
 909 fold-changes (FC) in transcription between blood-stages and salivary-gland sporozoites  
 910 relative to statistical significance threshold (False Discovery Rate (FDR)  $\leq$  0.05). Positive  
 911 FC represents enriched transcription in the sporozoite stage. **c** Mirror plot showing  
 912 pFam domains statistically significantly (FDR  $\leq$  0.05) over-represented in salivary-gland  
 913 sporozoite enriched (red) or blood-stage enriched (black) transcripts. Scale bar  
 914 truncated for presentation. \* - 55 PRESAN domains are in this dataset. \*\* - 99 Vir  
 915 domains are in this dataset.

916

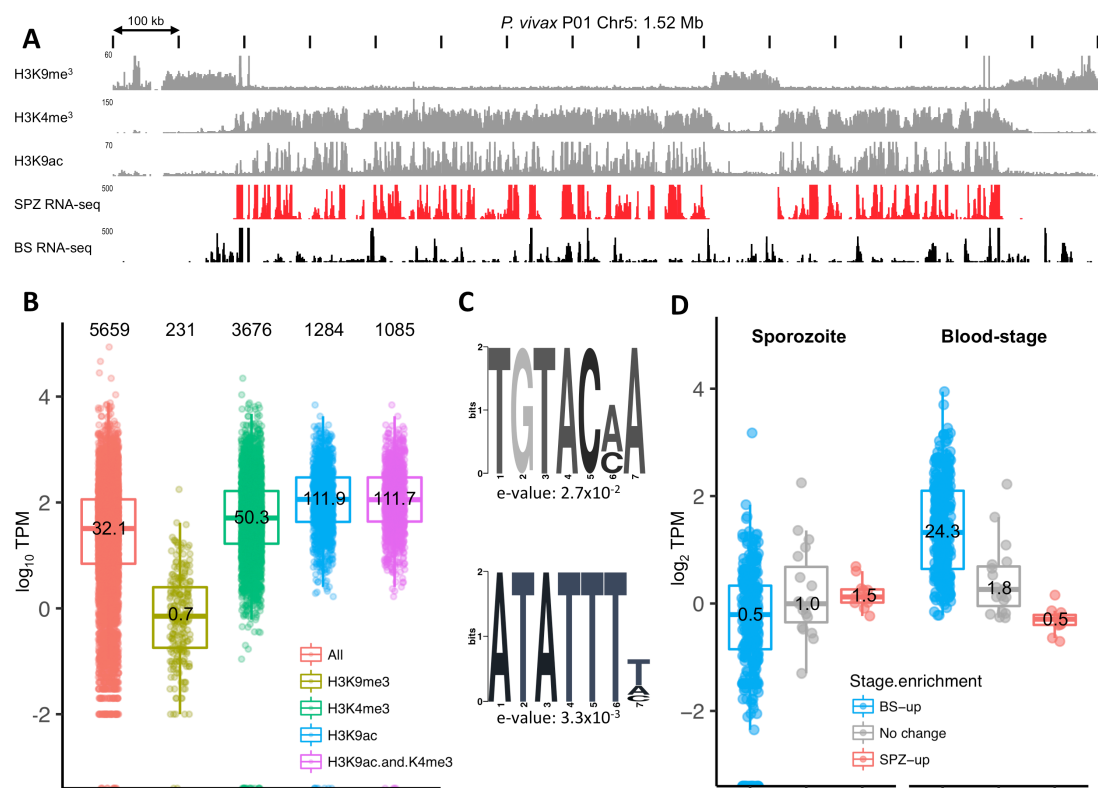


917

918

919  
 920  
 921  
 922  
 923  
 924  
 925  
 926  
 927  
 928  
 929  
 930  
 931  
 932  
 933  
 934

**Fig. 2** Histone epigenetics relative to transcriptional behaviour in salivary-gland sporozoites. **a** Representative H3K9me<sup>3</sup>, H3K4me<sup>3</sup> and H3K9ac ChIP-seq data (grey) from a representative chromosome (*P. vivax* P01 Chr5) relative to mRNA transcription in salivary-gland sporozoites (black) and blood-stages (black). Small numbers to top left of each row show data range. **b** Salivary-gland sporozoite transcription relative to nearest stable histone epigenetic marks. Numbers at the top of the figure represent total genes included in each category. Numbers within in box plot represent mean transcription in transcripts per million (TPM). **c** Sequence motifs enriched within 1kb upstream of the Transcription Start Site of highly transcribed (top 10%) relative to lowly transcribed genes associated with H3K9ac marks in salivary-gland sporozoites. **d** Relative transcription of (sub)telomeric genes in *P. vivax* salivary-gland sporozoites and blood-stages categorized by gene sets enriched in blood-stages (blue), salivary sporozoites (red) or not stage enriched (grey). Numbers in each box show mean transcription in TPM.



935  
 936

